JOURNAL OF CATALYSIS **175,** 129–134 (1998)
ARTICLE NO. CA981963

Behavior of MoS_2 Intercalation Compounds in HDS Catalysis

Keenan E. Dungey, M. David Curtis, and James E. Penner-Hahn

Willard H. Dow Laboratory, Department of Chemistry, The University of Michigan, Ann Arbor, Michigan 48109-1055

Received May 1, 1997; revised November 10, 1997; accepted November 11, 1997

MoS_2 intercalated with various proportions of $Co(OH)_2$ or Cp_2Co^+ were used as catalyst precursors for the hydrodesulfurization of thiophene in a differential flow reactor. X-ray diffraction and EXAFS were used to characterize the structures of the pristine and used catalysts. It was shown that the intercalates are unstable under the reaction conditions and revert to 2H-MoS_2 with extrusion of the intercalated material, which is then converted to Co_9S_8. The catalytic activity, normalized to the BET surface area, and the product distributions at steady state are essentially identical to conventionally prepared, Co-promoted MoS_2. It is argued that the pseudo-intercalation theory does not model the active site. © 1998 Academic Press

The catalytic hydrodesulfurization (HDS) of petroleum has been practiced for 50 years, but the nature of the active site has yet to be elucidated (1). The commercial catalyst consists of MS_2 supported on alumina and promoted by M' (M = Mo, W; M' = Co, Ni). The complexity of this mixture can be seen in the fact that over 30 models for the promotion effect have been proposed in the literature and at least 4 of these are still under debate. In the anion vacancy model, loss of sulfide ions in chains of MoS_2 forms the active site, with the role of Co being to stabilize the chains (2). A model involving the partial intercalation of Co^{+2} ions into octahedral sites between layers of MoS_2, called pseudo-intercalation (3), was proposed by Farragher *et al.* Delmon *et al.* proposed a model in which the interface between an MoS_2 particle and a Co_9S_8 particle forms the active site (4). In this model, called contact synergy, the role of the Co phase is to provide surface hydrogen (hydrogen spillover). Recently, Topsøe *et al.* detected a new Co–Mo–S phase by Mössbauer (5), in which the Co atoms are thought to decorate the edges of MoS_2 platelets.

Although structural and catalytic studies have been directed toward the contact synergy (6) and Co–Mo–S models (7), the only evidence for the pseudo-intercalation model is the analogy with known intercalation compounds of transition metal sulfide hosts, such as NbS_2 (8). The pseudo-intercalation model has not been tested previously by direct intercalation of MoS_2 by Co. Due to the electronic structure of 2H-MoS_2, direct intercalation is not possible except by strongly reducing agents, such as alkali metals (9), which induce a structural change (10). Furthermore, intercalation alters the electronic structure of the MoS_2 layer and it was of interest to determine the effect of the altered electronic state on HDS activity. At high temperatures, Group VIII ions can diffuse through the basal planes of MoS_2 to form intercalates, but this results in low surface area materials (11). Catalytic studies of the structurally characterized ternary phase, $CoMo_2S_4$ (12), reported that this material was not very active for HDS, though whether this was due to low surface area was not explained (13). In an attempt to intercalate some form of cobalt into MoS_2, Blekken *et al.* reacted cobaltocene (Cp_2Co, $Cp = \eta^5$-C_5H_5) with MoS_2 (14). Although it has an ionization potential similar to that of Li, the Cp_2Co did not intercalate due to steric constraints.

Recently, a method of synthesizing intercalation compounds of MS_2 has been devised that entails the exfoliation of Li-intercalated MS_2 in H_2O in the presence of a guest (15). The methanation activity of supported materials produced by this method was determined, but no hydrodesulfurization activity has been reported (16). Herein is described the behavior of a series of Co complexes intercalated into MoS_2 under HDS conditions. Structural changes during the catalysis, as determined *ex situ* by powder XRD and X-ray absorption spectroscopy, demonstrated the instability of MoS_2 intercalates under typical HDS reaction conditions.

Synthesis of the intercalation complexes is described elsewhere (17). Briefly, a colloidal suspension of MoS_2 single layers was made by reacting $LiMoS_2$ (**1**) with H_2O in a sonication bath. This suspension was added to aqueous solutions of $Co(OH_2)_6(NO_3)_2$ (**3a**, **b**), $Co(NH_3)_6Cl_3$ (**4**), and Cp_2CoCl (**5**) which induced flocculation. The colloidal suspension could also be acidified, causing flocculation and precipitation of restacked MoS_2 (**2**). A portion of **2** was heated in air for 10 min at 160°C (**2 ht**) while another sample was aged in air at room temperature for 2 months (**2 old**). The characterization of these materials is summarized in Table 1. The amount of Mo and Co in each sample was determined by electron microprobe analysis (EMPA), performed at the Electron Microscopy Analysis Laboratory at the University of Michigan, and surface areas were

0021-9517/98 $25.00

TABLE 1

Catalyst Characterization

Sample number[a]	Formula unit	Co source[b]	At.% Mo	At.% Co	Area[c] (m^2/g)
MoS_2	MoS_2	None			6
2[d]	MoS_2	None			52
3a	$[Co(OH)_2]_{0.27}MoS_2$	$Co(OH_2)_6(NO_3)_2$	51.78	13.80	20
3b	$[Co(OH)_2]_{0.57}MoS_2$	$Co(OH_2)_6(NO_3)_2$	46.13	26.21	20
4	$[Co(OH)_2]_{0.76}MoS_2$	$Co(NH_3)_6Cl_3$	41.82	31.74	34
5	$[Cp_2Co]_{0.14}MoS_2$	$[Cp_2Co]Cl$	51.06	7.22	11

[a] Samples used for HDS catalysis have the same number proceeded by the letter "U."

[b] Co complex used as Co source for intercalation.

[c] Surface area determined by single-point BET.

[d] Exfoliated and restacked MoS_2.

determined by single-point BET on samples degassed in H_2 for 3 h at 400°C on a Quantasorb instrument.

Catalytic activity of the materials for HDS of thiophene was measured in a fixed-bed microreactor operating in differential mode at 101 kPa. Products were analyzed by GC (PE 8400, $8' \times 1/8''$ 0.19% picric acid on Carbopack-C) and quantified by a standardized gas mix (Scott Specialty Gases). The fritted glass reactor (0.5 cm i.d.) was packed with 0.1 to 0.5 g of catalyst. The catalysts were degassed at 270°C in He (20 cm^3/min) for 1.5 h, and then the carrier gas was switched to H_2 (5–10 cm^3/min) and thiophene introduced via a bubbler/ice bath saturator (thiophene pressure, 20 Torr at 0°C). Steady state was achieved in approximately 4 h and then data from three to four GC runs were collected and averaged. To estimate the activation energy, the activity was determined at five different temperatures in 15°C increments.

Powder X-ray diffraction patterns of air-stable materials were taken on a Philips diffractometer, a Rigaku θ-θ diffractometer, or a Rigaku Rotaflex with Cu $K\alpha$ radiation. The used catalysts were treated as air-sensitive compounds and the samples were affixed to glass slides via double-sided tape in an inert atmosphere box, then sealed under more tape, and transferred to the diffractometer in vials. Silicon powder (National Bureau of Standards) was added to the samples as a standard for XRD spacing. X-ray absorption spectra were measured at 10 K at the Stanford Synchrotron Radiation Laboratory (SSRL) on beam line II-3, with synchrotron energies of 3.0 GeV and a stored current of 100 mA. Experimental details are given elsewhere (17), and the data were analyzed according to standard procedures (18).

The structure of the intercalation compounds has been explored and will be reported in detail elsewhere (17). Briefly, however, exfoliation of $LiMoS_2$ upon reaction with water results in a suspension of single layers of MoS_2 that remain partially negatively charged. These single layers have a 1T-MoS_2 structure: the Mo atoms are octahedrally coordinated by S and there is an intralayer distortion in which the Mo atoms cluster in a manner similar to the Re atoms in $ReSe_2$ (19), yielding long and short Mo–Mo distances. When these single layers are discharged by reaction with a metal cation or with H^+, the layers coagulate and form "restacked" MoS_2. This restacked MoS_2 initially retains the 1T-MoS_2 distortion, but this structure is metastable and reverts back to stable 2H-MoS_2 upon standing at room temperature or (more rapidly) with heating (**2 old** and **2 ht** in Table 3, respectively). The interlayer spacing of 1T-MoS_2 and 2H-MoS_2 are essentially identical (c = 6.14 Å = d_{002} in 2H-MoS_2). Thus, samples of MoS_2 intercalates, e.g. $(Cp_2Co)_{0.14}MoS_2$ (**5**), while exhibiting a single interlayer spacing by XRD may have both distorted and undistorted MoS_2 layers, with the relative amount of each depending upon the sample's age and thermal history.

Thus, Fig. 1a shows the Fourier transform of the Mo K-edge EXAFS of **5**, in which there are four scattering shells corresponding to distorted and undistorted MoS_2 layers. The first can be fit with six sulfur atoms at 2.42 Å, which is the Mo–S distance in 2H-MoS_2. The next three shells can be fit with Mo atoms at 2.78, 3.16, and 3.78 Å. The middle Mo–Mo distance is the same as that in undistorted 2H-MoS_2, while the presence of Mo atoms at the shorter

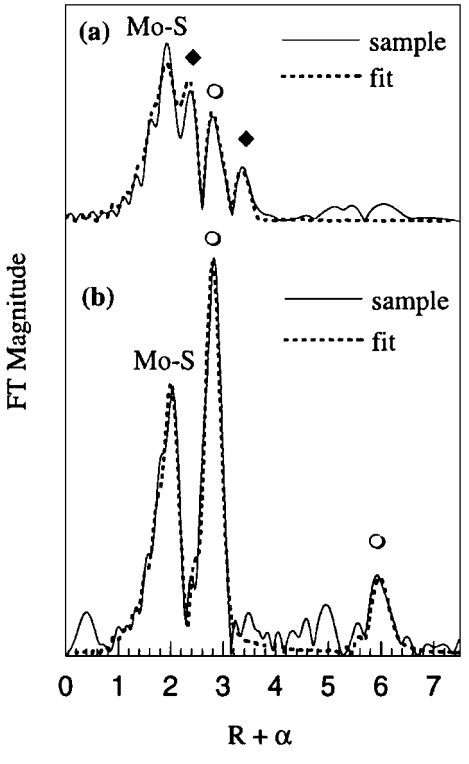

FIG. 1. FT of Mo EXAFS for (a) $[Cp_2Co]_{0.14}MoS_2$ (**5**) showing different Mo peaks due to the presence of 2H-MoS_2 (○) and distorted MoS_2 (◆) phases, (b) **U5**.

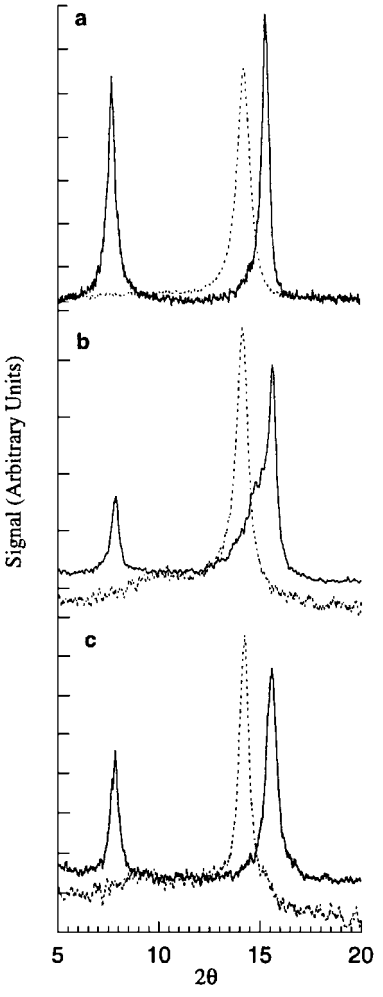

FIG. 2. Powder X-ray diffraction patterns of (a) $[Cp_2Co]_{0.14}MoS_2$ (**5**), (b) $[Co(OH)_2]_{0.27}MoS_2$ (**3a**), and (c) $[Co(OH)_2]_{0.76}MoS_2$ (**4**) before (solid) and after (dashed) catalysis, showing conversion to 2H-MoS_2.

and longer distances are indicative of the charge density wave in the $ReSe_2$-type distorted MoS_2 layers.

On the other hand, the powder X-ray diffraction patterns of the intercalates (Fig. 2, solid lines) show only 001 and 002 diffraction peaks at $2\theta = 7.7$ and 15.4° that correspond to *d* spacings of 11.3 and 5.7 Å, respectively. These are quite distinct from the 002 peak of 2H-MoS_2 at $2\theta = 14.4°$. Thus, intercalation of either Cp_2Co or $Co(OH)_2$ causes an expansion between the MoS_2 layers of approximately 5.2 Å, but some of the MoS_2 layers have the 1T-MoS_2 distortion, while some have the 2H-MoS_2 structure. Co *K*-edge EXAFS data show that the Co–Cp bonding is retained in the Cp_2Co intercalate (**5** in Fig. 5), but a single, intercalated layer of $Co(OH)_2$ is formed from either $[Co(OH_2)_6]^{+2}$ (20) or $[Co(NH_3)_6]^{+3}$.

The catalytic activity of the intercalation compounds of MoS_2 toward the hydrodesulfurization of thiophene was studied. Table 2 summarizes the reaction rates, Arrhenius parameters, and product distributions for all of the catalysts at steady state. As the materials were not pretreated (e.g., sulfided and/or reduced) there was an initial period of instability in the reaction rate, as shown in Fig. 3. Normally, HDS catalysts require an activation period, where the activity increases with time-on-stream, as the catalyst is sulfided. This activation behavior is demonstrated with $(Cp_2Co)_{0.14}MoS_2$ (**5**), but the opposite behavior is observed for the $Co(OH)_2$ intercalation compound, **3a**. The activity slightly decreases, suggesting that the initial intercalation compound is more active than the steady-state catalyst.

The normalized reaction rates for the materials are on the order of nanomoles of thiophene converted per square meter of surface per second. These rates are three orders of magnitude less than typical supported, promoted MoS_2 HDS catalysts (7a, 21). This vast difference in reaction rates is related to greater dispersion in the supported catalysts. In general, the number of active sites is proportional to the surface area. However, MoS_2 in the supported catalyst is dispersed as single layers of MoS_2 (22), and this material has more defects than crystalline, multi-stacked MoS_2. Therefore, the number and (to some extent) the quality of the active site will be different in the supported versus unsupported catalysts, and the activities of supported and crystalline MoS_2 cannot be compared in a meaningful way.

By plotting the relative HDS reactivity rates at 573 K (normalized per surface area) versus the cobalt/molybdenum ratio (as determined by EMPA), a Co promotion factor is observed (Fig. 4). The activity increases by about a factor of four, with the maximum activity near the Co/(Co + Mo) ratio of 0.4. This promotion is slightly less than that previously observed in supported Co/MoS_2 catalysts (23).

The apparent activation energies for the HDS of thiophene with the catalysts were calculated from Arrhenius

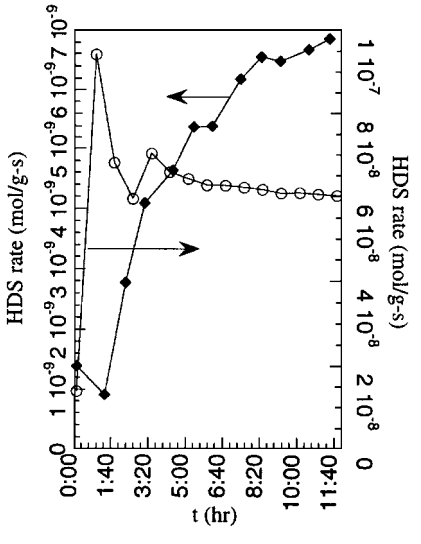

FIG. 3. Change in initial HDS rates for $[Cp_2Co]_{0.14}MoS_2$ (**5**) (◆) and $[Co(OH)_2]_{0.27}MoS_2$ (**3a**) (○), operating at 543 and 573 K, respectively.

TABLE 2

HDS of Thiophene at 573 K by MoS_2 Intercalation Compounds

Catalyst	H_2 flow (cm^3/min)	Rxn rate (nmol/m^2 s)	% Conv.	ΔE_a[a] (kcal/mol)	Propene (pmol)	Butane (pmol)	*i*-butene (pmol)	1-butene (pmol)	*c*-butene (pmol)	*t*-butene (pmol)	Butadiene (pmol)
MoS_2	10	0.56	1.47	15.6 ± 0.9	156	122	89	677	355	406	108
mol%					8	6	5	35	18	21	6
2	5	1.19	10.0	16.4 ± 1.7	245	7120	563	1075	1482	2353	54
mol%					2	55	4	8	11	18	0.4
3a	10	2.55	7.4		101	761	0	2840	2476	3481	112
mol%					1	8	0	29	25	35	1
3b	10	4.25	7.15	17.1 ± 1.7	226	388	119	3372	2051	2620	72
mol%					2	4	1	38	23	30	1
4	10	3.71	18.16	18.0 ± 1.8	179	2045	193	4948	6839	10550	0
mol%					1	8	1	20	28	42	0
5	10	1.27	1.6	17.8 ± 2.6	153	319	318	382	312	527	42
mol%					7	16	16	19	15	26	2

[a] Calculated from the linear regression of Arrhenius plots.

plots (with linear regression correlation factors of 0.97 to 0.99) and found to be the same value within the error of the measurements (17 ± 2 kcal/mol). This activation energy is similar to what has been observed for other HDS catalysts (24) and implies that the same rate-controlling step is involved. It is interesting to note that the same energy of activation is observed for both the promoted and unpromoted catalysts.

The structures of the used, steady-state catalysts were determined by X-ray diffraction and X-ray absorption. The only diffraction peaks present in the used catalysts were those due to 2H-MoS_2 (Fig. 2, dashed lines, $2\theta = 14.4^\circ$). EXAFS data on the used catalysts were also consistent with 2H-MoS_2 as the only detectable Mo-phase present (Fig. 1b, Table 3). There are two scattering shells at low *R* (<4 Å), corresponding to six sulfur atoms at 2.42 Å and six molybdenum atoms at 3.16 Å. In addition, a longer *R* shell can be fit with Mo at 6.4 Å, corresponding to Mo atoms in neighboring MoS_2 sheets.

The local structure around the Co also changes dramatically after these materials are used as HDS catalysts. Figure 5 compares the Fourier transforms of the Co EXAFS for the used catalysts with that of Co_9S_8, using the same *k* space region (3–12 $Å^{-1}$). Most of the samples have the same broad peak at an $R + \alpha$ of 2 Å, which is actually two unresolved scattering shells. The first shell can be fit with sulfur atoms at a distance of 2.2 Å from the absorbing cobalt, while the second shell corresponds to cobalt atoms at a distance

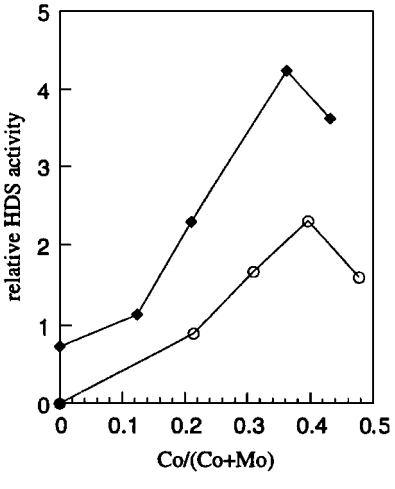

FIG. 4. HDS activity relative to MoS_2 from (◆) this study and (○) Ref. (23).

TABLE 3

Fitting Parameters for Mo *K*-Edge EXAFS of Used Catalysts[a]

Sample	Mo–S			Mo···Mo			*F*
	N	*R* (Å)	σ^2 ($Å^2$)	*N*	*R* (Å)	σ^2 ($Å^2$)	
MoS_2	6.0	2.42	2.8	6.0	3.16	1.6	0.058
$UMoS_2$	5.7	2.41	2.8	5.1	3.17	1.6	0.110
U2	5.3	2.41	2.8	3.4	3.16	1.6	0.045
2 ht[b]	5.4	2.41	2.8	3.1	3.16	1.6	0.030
2 old[c]	4.6	2.41	2.8	2.7	3.16	1.6	0.029
U3a	5.5	2.41	2.8	3.7	3.16	1.6	0.043
U4	5.4	2.40	2.8	3.3	3.16	1.6	0.035
U5	5.7	2.41	2.8	3.7	3.16	1.6	0.038
MoS_2, xtl[d]	6.0	2.42		6.0	3.16		

[a] *N* is the number of scatterers, *R* is the absorber–scatterer distance in Å, σ^2 is the Debye–Waller factor in $Å^2 \times 10^3$ for each shell, which has been fixed to the values for MoS_2 (2.8 and 1.6 $Å^2 \times 10^3$). $F = ([\sum(\chi_{obs} - \chi_{calc})^2]/[N_{pts} - N_{var}])^{0.5}$ goodness of fit index. The threshold energy (E_0) for all shells in all fits was 24.0 eV, while the scale factor was set to 1.1.

[b] 2H-MoS_2 formed by heating freshly exfoliated and restacked MoS_2.

[c] 2H-MoS_2 formed by slow transformation of 1T-MoS_2 after 2 months at room temperature.

[d] Crystal data for 2H-MoS_2 from Ref. (29).

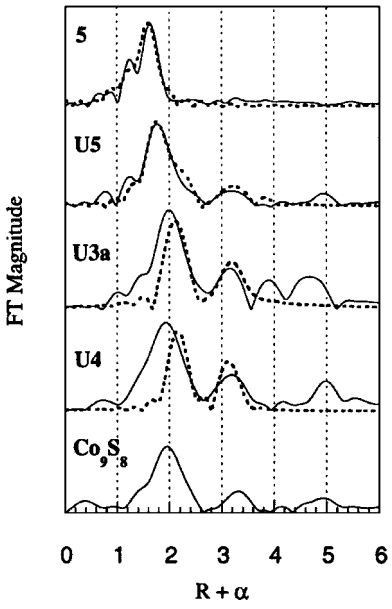

FIG. 5. FT of Co EXAFS for $[Cp_2Co]_{0.14}MoS_2$ (**5**), **U5**, **U3a**, **U4** and Co_9S_8 with k range fixed at 3–12 $Å^{-1}$. The solid lines are the raw data while the dashed lines are the calculated fits, which do not fit well due to an unresolved S shell, explained in Table 4.

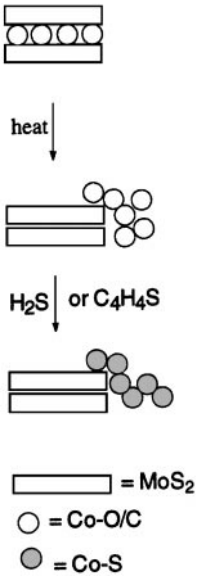

SCHEME 1

of 2.5 Å. Another cobalt shell is present at 3.50 Å. As can be seen in Table 4, the distances and coordination numbers are consistent with the tetrahedrally coordinated Co atoms found in Co_9S_8, the thermodynamically stable phase under these conditions (25). There is a shift in the first peak in the Fourier transform of the Co EXAFS for **U5** (Fig. 5), which is probably due to the fact that cobalt is more dispersed in this sample, so there is a smaller number of neighboring Co atoms.

These data show that under HDS reaction conditions, thermal decomposition of the intercalated MoS_2 occurs to give 2H-MoS_2 as the guest material is ejected. Since these extruded Co materials are now exposed to the reactor conditions, including H_2, thiophene, and H_2S (from the desulfurization of thiophene), Co_9S_8 is formed. These changes are illustrated in Scheme 1. These results show conclusively that bulk phases of Co-intercalated MoS_2 are not stable under HDS conditions. Furthermore, recent HREM results show that MoS_2 wets a surface of alumina, so that most of the Mo in commercial, supported catalysts is in the form of highly distorted single layers of MoS_2 with many folds, kinks, and other defects (1b, 22, 26). Relatively little MoS_2 exists in the form of multi-sheet stacks of the type that are necessary to form intercalates. These facts, when taken together, strongly suggest that even if traces of Co were to remain between the MoS_2 sheets in the minority phase (i.e., multilayered MoS_2), these structures are not responsible for the promotion effect observed in supported catalysts. The

TABLE 4

Fitting Parameters for Co *K*-Edge EXAFS of Used Catalysts[a]

	Co–S				Co···Co				Co···Co					
Sample	N	R	σ^2	s.f.	N	R	σ^2	s.f.	N	R	σ^2	s.f.	ΔE_o	F
U3a[b]					3	2.49	2.0	0.77	6	3.51	0.4	0.45	5.5	0.42
U4[b]	3	2.17	1061	0.85	3	2.49	2.4	0.62	6	3.50	1.5	0.42	5.0	0.104
U5	4	2.21	4.6	0.9	0.5	2.52	4.2	0.77	2.5	3.52	2.5	0.45	5.5	0.25
Co_9S_8[b]	4	2.19	876	0.85	3	2.50	3.8	0.62	6	3.50	1.9	0.2	5.0	0.090
Co_9S_8, xtl[c]	4	2.19			3	2.50			6	3.50				

[a] N is the number of scatterers, R is the absorber–scatterer distance in Å, σ^2 is the Debye–Waller factor in $Å^2 \times 10^3$ for each shell. $F = ([\sum(\chi_{obs} - \chi_{calc})^2]/[N_{pts} - N_{var}])^{0.5}$ goodness of fit index. s.f. is the scale factor for each shell. ΔE_o is the threshold energy in eV, which was the same for all the shells in a fit.

[b] Well-resolved S and Co shells were not possible using the computer fitting routine. The Co shell is only 0.3 Å from the S shell and therefore dominates the fit, resulting in an extremely large σ^2 for the S shell. There were not enough data points in **U3a** for an S shell fit.

[c] Crystal data for Co_9S_8 from Ref. (30).

notion that small amounts of highly active Co in a minority phase is simply not consistent with the observation that the maximum in the Co-promotion effect occurs at a high Co/Mo ratio (Co/Mo $\approx$ 0.7).

Our demonstration that Co intercalation structures are unstable under HDS conditions confirms the thermodynamic arguments against the pseudo-intercalation model (27). Furthermore, Mo/S species are mobile on alumina under HDS conditions, which means that the thermodynamically stable phase (2H-MoS_2) is kinetically accessible even in highly dispersed systems, such as discrete, supported clusters (28). As a result, the final structure of Al_2O_3-supported MoS_2 catalysts is essentially independent of the Mo precursor.

ACKNOWLEDGMENTS

This work was supported by the National Science Foundation under Grant CHE-9523056. We thank Prof. Levi Thompson for the use of the instruments in his laboratory for the BET measurements. K.E.D. is grateful to the Department of Chemistry and the College of Literature, Sciences, and Arts for a Regent's Fellowship.

REFERENCES

1. (a) Topsøe, H., Clausen, B. S., and Massoth, F. E., *in* "Catalysis–Science and Technology" (J. R. Anderson and M. Boudart, Eds.), Vol. 11. Springer-Verlag, New York, 1996; (b) Chianelli, R. R., Daage, M., and Ledoux, M. J., *Adv. Catal.* **40**, 177 (1994).
2. Lipsch, J. M. J. G., and Schuit, G. C. A., *J. Catal.* **15**, 179 (1969).
3. Farragher, A. L., and Cossee, P., *in* "Proceedings, 5th International Congress on Catalysis, Palm Beach, 1972" (J. W. Hightower, Ed.), p. 1301. North-Holland, Amsterdam, 1973.
4. Delmon, B., *in* "Proc. 3rd Int. Conf. on Chemistry and Uses of Molybdenum" (H. F. Barry and P. C. H. Mitchell, Eds.), p. 73. Climax Molybdenum, Ann Arbor, 1979.
5. Topsøe, H., and Clausen, B. S., *Catal. Rev. Sci. Eng.* **26**, 395 (1984).
6. Pirotte, D., Zabala, J. M., Grange, P., and Delmon, B., *Bull. Soc. Chim. Belg.* **90**, 1239 (1981).
7. (a) Bouwens, S. M. A. M., van Veen, J. A. R., Koningsberger, D. C., de Beer, V. H. J., and Prins, R., *J. Phys. Chem.* **95**, 123 (1991); (b) Bouwens, S. M. A. M., Prins, R., de Beer, V. H. J., and Koningsberger, D. C., *J. Phys. Chem.* **94**, 3711 (1990).
8. Van Den Berg, J. M., and Cossee, P., *Inorg. Chim. Acta* **2**, 143 (1968).
9. Thompson, A. H., and Di Salvo, F. J., *in* "Intercalation Chemistry" (M. S. Whittingham and A. J. Jacobson, Eds.), p. 573. Academic, New York, 1982.
10. Py, M. A., and Hearing, R. R., *Can. J. Phys.* **61**, 76 (1983).
11. Kamaratos, M., and Papageorgopoulos, C., *Solid State Commun.* **61**, 567 (1987).
12. Anzenhofer, K., and De Boer, J. J., *Acta Crystallogr. B* **25**, 1419 (1969).
13. Hagenbach, G., Courty, Ph., and Delmon, B., *J. Catal.* **23**, 295 (1971).
14. Blekkan, E. A., and Mitchell, P. V., *Bull. Soc. Chim. Belg.* **96**, 961 (1987).
15. Gee, M. A., Frindt, R. F., Joensen, P., and Morrison, S. R., *Mater. Res. Bull.* **21**, 543 (1986).
16. Miremadi, B. K., and Morrison, S. R., *J. Catal.* **103**, 334 (1987).
17. Dungey, K. E., Curtis, M. D., and Penner-Hahn, J. E., *Chem. Mater.*, submitted.
18. Teo, B. K., "EXAFS: Basic Principles and Data Analysis." Springer-Verlag, Berlin, 1986.
19. Alcock, N. W., and Kjekshus, A., *Acta Chem. Scand.* **19**, 79 (1965).
20. Valeev, E. F., Zubavitchus, Y. V., Slovokhotov, Y. L., Golub, A. S., Protzenko, G. A., and Novikov, Y. N., *Physica B* **208/209**, 569 (1995).
21. Browne, V. M., Louwers, S. P. A., and Prins, R., *Catal. Today* **10**, 345 (1991).
22. Stockman, R. M., Zandlbergen, H. W., van Langeveld, A. D., and Moulijn, J. A., *J. Mol. Catal. A. Chem.* **102**, 147 (1995).
23. De Beer, V. H. J., van Sint Fiet, T. H. M., Engelen, J. F., van Haandel, A. C., Wolfs, M. W. J., Amberg, C. H., and Shuit, G. C. A., *J. Catal.* **27**, 357 (1972).
24. Chianelli, R. R., Pecoraro, T. A., Halbert, T. R., Pan, W.-H., and Stiefel, E. I., *J. Catal.* **86**, 226 (1984).
25. (a) McKinley, J. B., *in* "Catalysis" (P. B. Emmett, Ed.), Vol. 5, p. 405. Reinhold, New York, 1957; (b) Rau, H., *J. Phys. Chem. Solids* **37**, 931 (1976).
26. Chianelli, R. R., Ruppert, A. F., Jose-Yacaman, M., and Vazquez-Zavala, A., *Catal. Today* **23**, 269 (1995).
27. Huisman, R., De Jonge, R., Haas, C., and Jellinek, F., *J. Solid State Chem.* **3**, 56 (1971).
28. Curtis, M. D., *in* "Transition Metal Sulfur Chemistry" (E. I. Stiefel and K. Matsumoto, Eds.), p. 154. American Chemical Society, Washington, DC, 1996.
29. Schönfeld, B., Huang, J. J., and Moss, S. C., *Acta Crystallogr. B* **39**, 404 (1983).
30. Alsen, N., *Geol. Foeren. i Stockholm. Foerh.* **47**, 19 (1925).